Chemistry & Biology, Vol. 11, 1395–1402, October, 2004, ©2004 Elsevier Ltd. All rights reserved. DOI 10.1016/j.chembiol.2004.08.007

A Polymorphic Pocket at the P10 Position Contributes to Peptide Binding Specificity in Class II MHC Proteins

Zarixia Zavala-Ruiz,[1,4] Iwona Strug,[2,4] Matthew W. Anderson,[3] Jack Gorski,[3] and Lawrence J. Stern[2,*]
[1]Department of Chemistry
Massachusetts Institute of Technology
Cambridge, Massachusetts 02139
[2]Departments of Pathology and Biochemistry and Molecular Pharmacology
University of Massachusetts Medical School
Worcester, Massachusetts 01655
[3]Blood Research Institute
Blood Center of Southeastern Wisconsin
Milwaukee, Wisconsin 53201

Summary

Peptides bind to class II major histocompatibility complex (MHC) proteins in an extended conformation. Pockets in the peptide binding site spaced to accommodate peptide side chains at the P1, P4, P6, and P9 positions have been previously characterized and help to explain the obtained peptide binding specificity. However, two peptides differing only at P10 have significantly different binding affinities for HLA-DR1. The structure of HLA-DR1 in complex with the tighter binding peptide shows that the peptide binds in the usual polyproline type II conformation, but with the P10 residue accommodated in a shallow pocket at the end of the binding groove. HLA-DR1 variants with polymorphic residues at these positions were produced and found to exhibit different side chain specificity at the P10 position. These results define a new specificity position in HLA-DR proteins.

Introduction

Major histocompatibility complex (MHC) proteins play an important role in the generation of immune responses by binding peptide antigens and presenting them at the cell surface for inspection by antigen receptors on T cells [1]. T cell recognition of MHC bound antigens is required for the generation of adaptive immune responses against pathogenic viruses, bacteria, and fungi, and for selection and maintenance of the large repertoire of circulating T cells. Class II MHC proteins are found in macrophages, B cells, dendritic cells, and other "antigen-presenting cells" of the immune system, where they bind peptides produced by endosomal proteolysis. The endosomal antigen-processing machinery results in a large variety of peptide antigens bound to class II MHC proteins, with an average length of 15–20 residues [2, 3]. Peptides bind to class II MHC proteins in an extended conformation, with up to 12 peptide residues in direct contact with the MHC peptide binding groove [4]. Pockets in the peptide binding groove are spaced to accommodate some of the peptide side chains, with the remainder held accessible for interaction with T cell receptors. In structures of human and mouse class II MHC proteins, pockets within the overall peptide binding site are found at the P1, P4, P6, and P9 positions, with smaller pockets at P3 and P7 (Figure 1A) [5–12]. Pockets are numbered along the peptide relative to a large hydrophobic pocket near the peptide binding site. These positions are consistent with experimentally determined peptide binding motifs, which indicate peptide sequence preferences at these positions [13, 14].

Class II MHC proteins are highly polymorphic in all species that express them. Over 400 alleles have been characterized for the β subunit of HLA-DRB, the most highly expressed of the three human class II MHC proteins [15]. (The α subunit is nonpolymorphic). Most of the polymorphisms can be found in positions that correspond to the residues lining the pockets within the peptide binding site. The allelic differences influence the peptide binding specificity of the various class II MHC alleles and thus determine allele-specific differences in the spectrum of peptides presented to the immune system. These differences have important consequences for susceptibility to autoimmune diseases, resistance to infection, vaccine efficacy, and rejection of transplanted organs and administered proteins [16]. In the common allelic variant HLA-DR1 (DRB1*0101), for example, the P1 pocket shows strong preferences for large hydrophobic residues (such as Tyr, Trp, Phe, Leu, and Ile), the P6 pocket prefers smaller residues (Gly, Ala, Ser, and Pro), and the P4 and P9 pockets tend to have weaker preferences for residues that have aliphatic character [14]. Algorithms designed to predict peptide binding affinities for HLA-DR1 and for other class II MHC allelic variants have been developed based on experimental peptide and phage display binding data together with the pattern of MHC-peptide side chain contacts observed in the crystal structures [17–20]. Generally, such approaches have considered only positions P1–P9 or a subset of these positions, although one report analyzed specificity at positions P1–P10 by using randomized peptide libraries [21].

A recent study of HLA-DR52a (HLA-DRB3*0101) bound to an integrin β3-derived peptide suggested a role for the P10 position in peptide binding [22], and a similar effect was observed in a systematic study of contributions of anchor and nonanchor positions to the overall peptide binding affinity of HLA-DR1 [23]. Here, we have investigated the structural basis for specificity at the P10 position of peptides bound to HLA-DR1. A newly described shallow pocket or shelf on the edge of the MHC peptide binding site interacts with peptide P10 side chains, and common MHC polymorphisms in this region alter the peptide side-chain specificity. These results suggest that the P10 position can play an important role in MHC peptide binding selectivity.

*Correspondence: lawrence.stern@umassmed.edu
[4]These authors contributed equally to this work.

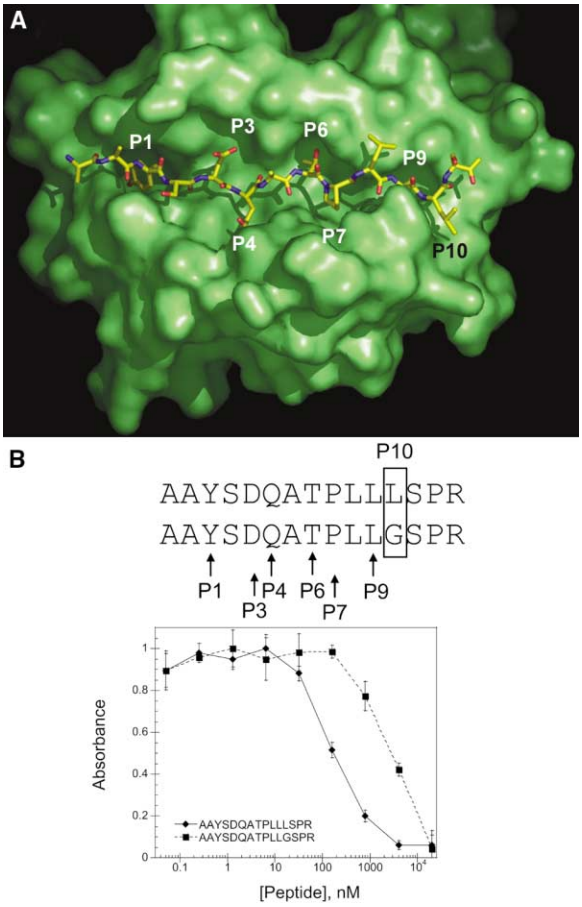

Figure 1. The P10 Position of Peptides Can Affect Binding to HLA-DR1

(A) Surface of the HLA-DR1 peptide binding site with bound AAYSD QATPLLLSPR peptide shown as a stick model. In the peptide, carbon atoms are yellow, nitrogen atoms are blue, and oxygen atoms are red. Peptide side chain binding pockets are labeled.

(B) Competitive binding analysis of two peptides that differ only in the P10 position. A fixed concentration of peptide-free HLA-DR1 and biotinylated Ha peptide was incubated with increasing concentrations of either AAYSDQATPLLLSPR or AAYSDQATPLLGSPR peptide. After binding for 3 days at 37°C, the amount of biotinylated Ha peptide/HLA-DR1 complexes was measured with alkaline phosphatase-labeled streptavidin in an antibody-capture assay.

Results and Discussion

The P10 Position Can Influence Binding of Peptides to HLA-DR1

Two peptides with sequences differing only by a single amino acid predicted to occupy the P10 pocket (AAYSD QATPLLLSPR and AAYSDQATPLLGSPR) bind to HLA-DR1 with 15-fold different apparent affinity as measured by a competition assay (Figure 1B). The peptide sequences derive from the integrin β3 peptide previously implicated in P10 effects in the context of HLA-DR52a [22], but with the "anchor" P1, P4, P6, and P9 positions changed to the corresponding residues from the influenza haemagglutin [306–318] peptide (HA), a well-characterized viral antigen that binds tightly to HLA-DR1 (Kd of ~10 nM) [12]. The difference in peptide binding affinity would appear to be due to an interaction between the peptide P10 residue and HLA-DR1. As noted above, a side-chain binding pocket at this position has not been described in HLA-DR1 or any other class II MHC protein, and peptide binding motifs generally do not include a side chain preference at this position. It is possible, however, that these peptides bind in an expected conformation, or that one (or both) of the peptides binds in an unexpected register or conformation; for example, the peptide might "bulge," as observed in complexes of peptides bound to class I MHC proteins [24], shifting the peptide side chains that are accommodated in the MHC pockets. To elucidate the structural basis for the apparent specificity at the P10 position, we crystallized HLA-DR1 in complex with the AAYSDQATPLLLSPR peptide and determined its structure by X-ray diffraction methods.

Crystal Structure of HLA-DR1 Reveals a P10 Shallow Pocket or Shelf

The X-ray crystal structure of HLA-DR1 bound to the AAYSDQATPLLLSPR peptide was determined in two crystal forms, one with two molecules in the asymmetric unit, and another with one molecule in the asymmetric unit in complex with the bacterial superantigen SEC3-3B2 that has been used previously to facilitate crystallization of HLA-DR variants (Table 1). SEC3-3B2 makes contacts with the α chain of HLA-DR1 outside the binding site and does not contact the peptide [25, 26]. In each of the structures, clear and continuous density was observed for essentially all of the MHC protein, excluding a disordered loop away from the peptide binding site, and also for all of the bound peptide from the P2 to P11 positions (Figures 2A and S1; see the Supplemental Data), excluding the P8 Leu side chain, which is oriented toward the T cell receptor and does not contact the MHC, and the Cδ1 and Cδ2 terminal methyl groups of the P10 Leu side chain. The peptide binds in the usual polyproline type-II conformation, using the expected anchor residues Tyr (P1), Gln (P4), Thr (P6), and Leu (P9) (Figure 2A). As commonly observed in class II MHC peptide structure, the peptide termini outside the binding site were disordered. The MHC and peptide portions of these structures were identical in the three views of the molecule provided by these crystals, except for some crystal contacts that vary between the crystals forms (Figure 2B). We were not able to obtain crystals of HLA-DR1 in complex with the other peptide (AAYSD QATPLLGSPR).

The peptide P10 residue and the area surrounding the MHC region were well-resolved in each of the crystal forms, with the exception of the terminal methyl groups of the P10 Leu. HLA-DR1 residues located in close proximity to the P10 side chain are Argα76, Proβ56, Aspβ57, and Tyrβ60 (Figure 2C). These residues form a shallow pocket or "shelf" that accommodates the P10 residue (Figure 2D). The interaction buries ~117 Å^2 of solvent accessible surface area from the Leu (P10) residue (of 1220 Å^2 that is buried from the entire peptide), and ~73 Å^2 of solvent accessible surface area from the MHC (of 850 Å^2 that is buried by interaction with the entire peptide). Essentially all of the MHC surface area buried

Table 1. Data Collection and Refinement Statistics

Crystal Parameters	HLA-DR1/AAYSDQATPLLLSPR		HLA-DR1/AAYSDQATPLLLSPR/SEC3-3B2	
Space Group	$C222_1$		R3	
Cell Dimensions a,b,c (Å)	96.55,112.65,172.75		173.21,173.21,121.54	
Data Collection	**Overall**	**Highest Res. Shell**	**Overall**	**Highest Res. shell**
Resolution limits (Å)	24.0–2.40	2.49–2.40	30.0–2.40	2.49–2.40
Unique reflections	44,505	4384	53,191	5,392
Total reflections	252,441	20,869	319,169	30,576
Completeness (%)	99.8	99.8	99.9	100.0
Mean I/σ (I)	11.0	3.5	9.7	2.0
R_{sym} (%)[a]	6.5	37.8	11.4	49.7
Refinement				
R_{free}[b]	25.6	38.1	24.1	34.9
R_{cryst}	23.1	31.8	20.8	31.2
Model	**Average B Factor (Å^2)**	**# Residues (Atoms)**	**Average B Factor (Å^2)**	**# Residues (Atoms)**
HLA-DR1	39.8	737 (6070)	39.9	368 (3027)
Peptide	51.5	26 (188)	47.4	13 (94)
SEC3-3B2	N/A	N/A	39.4	229 (1884)
Waters	40.9	166	42.0	287
Estimated Coordinate Error				
Luzatti (Å)	0.32		0.37	
Sigma A (Å)	0.31		0.34	
RMSD				
MHC (Å)	0.054[c]		0.28[d]	
Peptide (Å)	0.034[c]		0.24[d]	
Ramachandran Plot				
Core + Allowed (%)	99.7		99.8	
Generous (%)	0.0		0.2	

[a] $R_{sym} = \sigma|I - \langle I\rangle|/\sigma\langle I\rangle$, where I is the observed intensity and $\langle I\rangle$ is the average intensity of multiple observations of symmetry-related reflections.
[b] R factor on structure factors for reflection omitted from the refinement and used as a test set (10% of total).
[c] Relationship between the MHC or peptide components of the two NCS-related molecules in the asymmetric unit.
[d] Relationship between the MHC or peptide components of the R3 crystal form as compared to molecule 1 of the other crystal form. Values for molecule 2 are essentially identical

by the P10 residue is hydrophobic. The fraction buried for the residue at P10 is 0.63, which is comparable to the fraction buried for residues in the P3 (0.65), P4 (0.69), and P7 (0.77) pockets. Crystal structures are currently available for six other HLA-DR molecules in complex with peptides that extend to the P10 position. In each of these, the residues that line the P10 pocket are organized essentially identically to the complex reported here (Figure S2A; see the Supplemental Data). In each case, the P10 residue is substantially buried in the pocket (with the exception of DRB5*0101 in complex with a peptide from Epstein-Barr virus, where the peptide binds in an unusually extended conformation with the P9 residue contacting the P10 pocket) (Figure S2B).

Binding Specificity to the P10 "Shelf" on HLA-DR1

In order to explore peptide binding specificity for the P10 side chain, we synthesized a set of peptides that contained the AAYSDQATLLLXSPR sequence, where X is one of the 20 natural amino acids, and measured their relative affinity for HLA-DR1 in a competition binding assay (Figure 3A). The peptide sequence is similar to that used in the structural work described above, except that (P7) was changed to the more favorable Leu (P7), eliminating possible backbone conformational and entropic effects unique to proline (I.S., Z.Z.-R., and L.J.S., unpublished data). Peptide binding competition IC_{50} values are shown in Table S1 (see the Supplemental Data) and are plotted in Figure 3B relative to the average of all peptides in the series. Clearly there is peptide side chain specificity at the P10 position, with phenylalanine and tyrosine strongly preferred and asparagine, proline, and serine disfavored.

Allelic Polymorphism at the P10 Region of HLA-DR

Inspection of the HLA-DR1 structure in the vicinity of the P10 shelf shows that the residues Argα76, Proβ56, Aspβ57, and Tyrβ60 play the major roles in formation of the shelf and interaction with the peptide (Figures 2C and 2D). Argα76 is part of the nonpolymorphic α subunit, and Proβ56 is conserved within all the HLA-DR alleles,

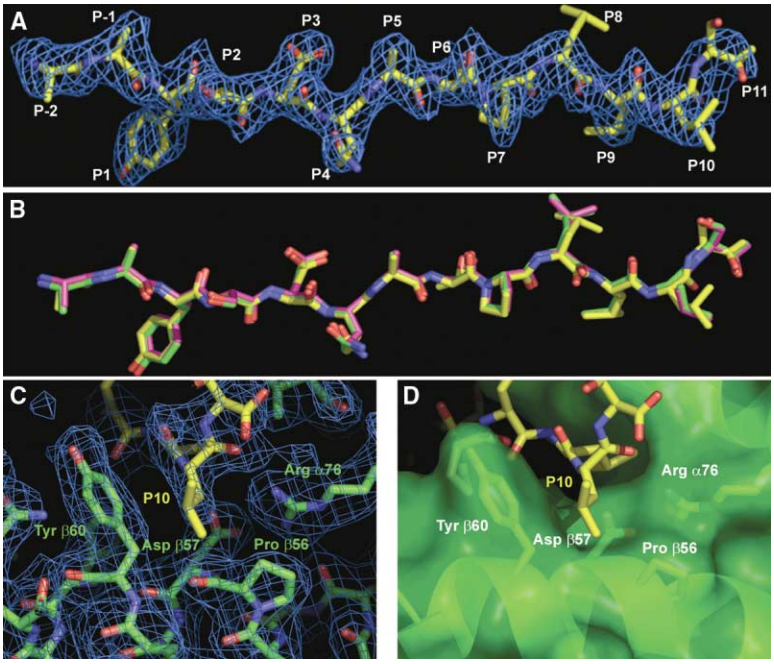

Figure 2. Crystal Structure of HLA-DR1 Bound to AAYSDQATPLLLSPR

(A) 2Fo-Fc electron density map contoured at 1σ using data in the resolution rage of 30–2.4 Å, with all peptide atoms omitted from the map calculation. The peptide carbon atoms are yellow, and nitrogen and oxygen atoms are blue and red, respectively.

(B) The AAYSDQATPLLLSPR peptide from the HLA-DR1/SEC3-3B2 complex (carbon atoms colored in yellow) was superimposed with the peptides present in the structure of HLA-DR1 without the superantigen (carbon atoms colored in green or magenta for the two molecules in the asymmetric unit).

(C) 2Fo-Fc electron density maps contoured at 1σ for the P10 region of HLA-DR1/AAYSD QATPLLLSPR. (All the labeled residues were omitted from the map calculation). The carbon atoms for the peptide are yellow, and the ones for HLA-DR1 are green. The view is from the right side of (A), with the α subunit helix to the right and the β subunit helix to the left.

(D) Surface of the HLA-DR1 P10 region shown with the same view as (C). Residues lining the pocket are labeled. Residues β57 and β60 are polymorphic among HLA-DR proteins. Figures were generated with PyMol [43].

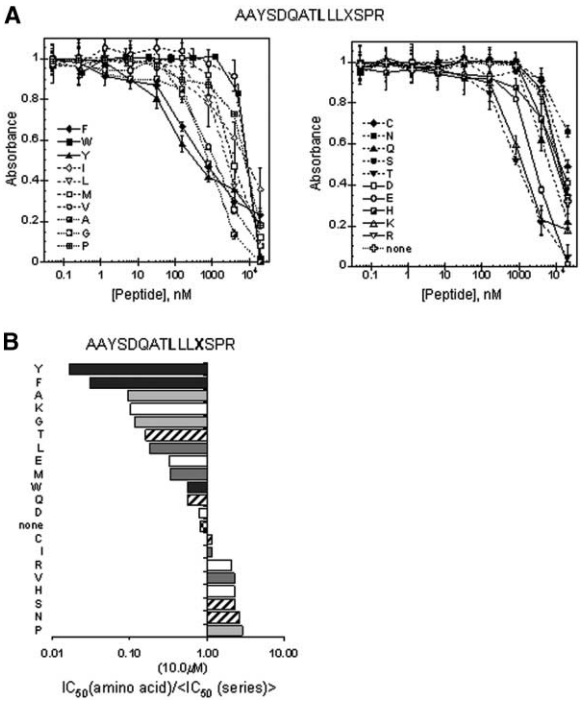

Figure 3. Effect of Different Amino Acids at the P10 Position of Peptides in Peptide Binding to HLA-DR1

(A) MHC-peptide binding competition assay of a set of peptides that contained the AAYSDQATLLLXSPR sequence, where X is one of the 20 natural amino acids.

(B) Effect of each amino acid at the P10 position. Values represent the IC_{50} of the residue over the average IC_{50} for the entire peptide series. The bar labeled "none" represents a peptide that ended at the P9 residue (this residue is amidated).

but Aspβ57 and Tyrβ60 are highly polymorphic (Table S2). In the context of other class II MHC proteins, polymorphism at Aspβ57 has been linked to human (HLA-DQ) and murine (I-A^{g7}) diabetes [5, 8].

We attempted to evaluate the effect of these polymorphisms on peptide side chain specificity at the P10 position by using published studies. The influence of β57 and β60 on HLA-DR peptide binding specificity has been studied systematically as part of a pocket-based matrix approach to epitope prediction [17], but the P10 pocket was not included in the analysis. For I-A^{g7}, a mouse class II MHC protein, it has been suggested that polymorphism at β57 can effect side chain preference at both the P9 and P10 positions [27]. Lists of peptides known to bind to particular human MHC alleles, and predicted allele-specific peptide binding motifs, have been collected in several databases, although quantitative data on the MHC-peptide binding interaction are not included [18, 19]. We scanned one such database, SYFPEITHI, for sets of similar HLA-DR1 alleles that differ in the P10 pocket residues β57 and β60 and for which reliable peptide binding motifs were available. DRB1*0401, DRB1*0404, and DRB1*0405 form such a set. These alleles differ only at positions β57 (Asp or Ser), β71 (Arg or Lys), and β86 (Gly or Val) (Figure 4). The polymorphism at β71 is not expected to significantly influence peptide side chain specificity, as both Argβ71 and Lysβ71 form a similar hydrogen bond with the peptide main chain carbonyl at position 5, between the P4 and P6 pockets [7, 12]. Residue β86 is found on the wall of the P1 pocket, and this polymorphism is expected to influence only the specificity at the P1 position [12, 17, 28]. Thus, the pattern of substitutions at these positions allows the effects of the Asp/Ser polymorphism at β57 to be evaluated: preferences observed for DRB1*0405 that are not shared by DRB1*0401 and DRB1*0404 can be attributed to the presence of Serβ57. The peptide binding motif

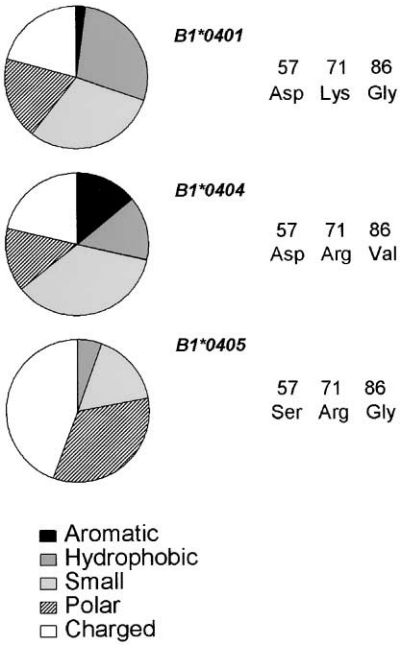

Figure 4. Analysis of Peptides that Bind to Different MHC Alleles

The frequencies of different groups of amino acids at the P10 position were calculated by using a list of peptides known to bind to DRB1*0401, DRB1*0404, and DRB1*0404 from the SYFPEITHI database [18]. The aromatic group includes Trp, Tyr, and Phe; the hydrophobic group includes Ile, Leu, Val, and Met; the small group includes Ala, Pro, and Gly; the polar group includes Thr, Ser, Cys, Asn, and Gln; and the charged group includes His, Glu, Arg, Lys, and Asp. Sequence differences between the three alleles are indicated; only β57 is in the P10 regions (each of the alleles has Tyrβ60).

for HLA-DR4 has been studied extensively [14, 17], allowing us to align a moderately sized set of known binders comprising 42 DRB1*0401 binding peptides, 14 DRB1*0404 binding peptides, and 17 DRB1*0405 binding peptides, according to their expected peptide binding frame. In this analysis, we included only peptides for which a single dominant binding register was apparent (Table S3). While the databases do not contain quantitative binding data on these peptides, it is evident that the alleles have selected sets of peptides that differ in the residue predicted in the P10 position, with the HLA-DRB1*0405 binding set enriched in charged amino acid residues at the expense of hydrophobic and aromatic residues (Figure 4). Thus, the β57 polymorphism appears to influence the P10 peptide binding specificity.

HLA-DR1 with Polymorphic Substitutions in the P10 Region Exhibits Altered P10 Specificity

To evaluate in a more quantitative way the influence of HLA-DR polymorphic residues on P10 specificity, we constructed a series of P10 pocket variants of HLA-DR1 (DRB1*0101) and evaluated their binding to the P10 peptide libraries as described above. Single and double amino acid replacements of polymorphic residues in the P10 shelf (βD57A, βD57A/Y60H, βD57V, and βD57V/Y60S) were introduced into HLA-DR1 so that their effects on P10 binding specificity could be isolated (naturally polymorphic variants at these positions also have substitutions in other pockets, like the HLA-DRB1*04 set described above). The resulting proteins were produced by expression in *E. coli* inclusion bodies and in vitro folding in the absence of peptide. The mutants were characterized to ensure that the substitutions did not result in gross alterations to the structure or to the peptide binding activity. First, each of the mutants exhibited a peptide-dependent decrease in gel filtration elution volume (Figure S3A), which previously has been described for HLA-DR1. The change results from a conformational alteration that accompanies the peptide as the binding site converts from a more open empty form to a more tightly packed closed form in the presence of peptide [29]. Second, each of the mutants bound the HA peptide (P10 Ala) with essentially identical apparent affinity (Figure S3B). Each of the mutants was also able to bind the CLIP peptide, a fragment of the class II-associated invariant chain that associates with class II MHC proteins during biosynthesis and intracellular trafficking. Apparent affinities for CLIP (P10 Gln) were similar but not identical, with D57V and D57V/Y60S binding more weakly (~3 fold). Thus, the mutations do not appear to have grossly altered the fold or activity of HLA-DR1.

To assess the effects of introduction of polymorphic residues in the P10 pocket on the peptide binding affinity and specificity at the P10 position, peptide binding competition assays were done for each mutant by using the AAYSDQATLLLXSPR series (Figure 5, Table S4). To facilitate comparison with the HLA-DR1 preferences, the bar graphs in Figure 5 are shown in the same order as in Figure 3D. Clear differences were observed between the P10 side chain specificities of the HLA-DR1 variants. For example, asparagine at the P10 position promotes binding to the βD57A/Y60H and βD57V/Y60S variants but significantly decreases binding in HLA-DR1 βD57A and βD57V variants. Some general preferences are apparent for the entire set; for example, Phe, Leu, Trp, and Met bind well, while Ile and His bind poorly to each of the variants.

Significance

MHC genes are the most polymorphic in the human genome. This polymorphism results in different peptide binding specificities for the corresponding allelic variant proteins. Thus, different individuals will react differently to a set of peptides from a particular antigen, with implications for vaccine design and susceptibility to autoimmune and infectious diseases. Algorithms that predict peptide binding to common human allelic variants are available and have found use in the study of autoimmune target antigens, in the design of immunogenic and nonimmunogenic protein therapeutics, and in development of subunit-based vaccines. For HLA-DR proteins, the most prevalent type of human class II MHC protein, such approaches generally account only for specificity at the P1–P9 positions of peptide antigen. Here, we have investigated an interaction outside this region, at the P10 position, which contributes significantly to the overall peptide binding affinity. In a crystal structure of HLA-DR1 bound to a

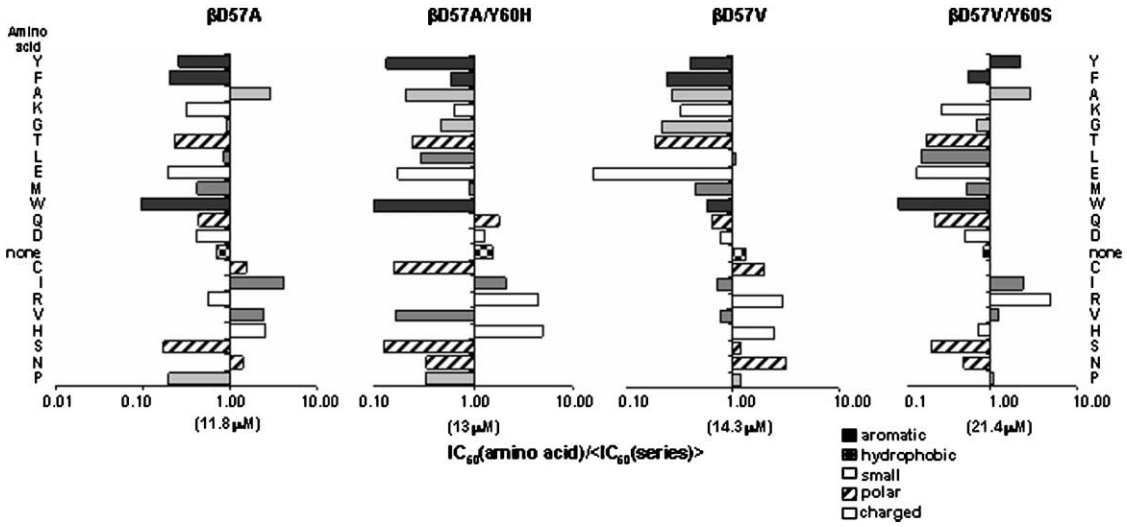

Figure 5. Influence of Different Amino Acids at the P10 Position in Peptide Binding to HLA-DR1 Mutants

Values represent the IC_{50} of the residue over the average IC_{50} of the entire AAYSDQATLLLXSPR peptide series for that particular HLA-DR1 mutant. The bar labeled "none" represents a peptide that ended at the P9 residue (this residue is amidated).

peptide antigen, we observed a shallow pocket that accommodates the P10 side chain. The residues that line this pocket are polymorphic among human HLA variants. We prepared HLA-DR1 variants carrying the polymorphic residues and analyzed their peptide binding specificity. Amino acid changes at the P10 position resulted in changes up to 50-fold in the apparent peptide binding affinity as measured by a competition assay. The P10 side chain binding specificity was significantly different for HLA-DR1 and for each of the variants. These results provide new data on peptide selection by human class II MHC proteins and should improve our ability to predict MHC allele-specific peptide binding patterns and individual differences in immunogenicity of protein therapeutics, autoimmune antigens, and vaccines.

Experimental Procedures

Peptide Synthesis

Peptides were synthesized by using solid-phase F-moc (N-[9-fluorenyl]methoxycarbonyl) chemistry on a Symphony instrument (Protein Technology, Inc.). All peptides were amidated at the C terminus. N-biotinylated peptides were prepared by coupling aminocaproyl-(LC)-biotin (Anaspec) to the N terminus of the resin bound, side–chain-protected peptide by using a standard amino acid coupling procedure. The peptides were deprotected and cleaved from the resin by a 2 hr treatment at room temperature with a mixture of trifluoroacetic acid/H_2O/thioanisole/phenol/dithiothreitol (82.5:5:5:5:2.5). The solution of peptides was precipitated with cold diethyl ether, and the crude peptides were filtered, washed with ether, and dried in vacuum. The crude peptides were purified by high-performance liquid chromatography (Vydac-C18). The purity and homogeneity of each peptide was checked by high-performance liquid chromatography (Vydac-C18) and MALDI-TOF mass spectrometry. Peptide concentrations were measured by absorbance at 280 nm ($\in_{280nm}$ = 1280 M^{-1} cm^{-1}) in the case of peptides containing tyrosine or weredetermined by using amino acid analysis in the case of CLIP peptide.

Protein Expression and Purification

For peptide binding experiments and X-ray crystallography, the extracellular portion of HLA-DR1 was produced from S2 (Schneider cell) insect cells as soluble empty $\alpha\beta$ heterodimers, as described previously [30]. For X-ray crystallography of the MHC-peptide complex in the presence of the superantigen, the extracellular portion of HLA-DR1 was produced by expression of isolated subunits in *Escherichia coli* inclusion bodies, followed by refolding in vitro as described previously [31]. Refolded HLA-DR1 was purified by immunoaffinity chromatography by using the conformation-specific monoclonal antibody LB3.1, followed by gel filtration chromatography in phosphate-buffered saline (pH 6.8). The protein concentration was measured by UV absorbance at 280 nm by using ϵ_{280} of 54,375 M^{-1} cm^{-1} for empty HLA-DR1. SEC-3B2 superantigen was expressed as a soluble protein in *E. coli* and isolated from the periplasmic fraction as described previously [32].

Construction and Analysis of HLA-DR1 Variants Carrying Single or Double Amino Acid Substitutions in the P10 Shelf

We used in vitro site-directed mutagenesis to make single or double point mutations on the β chain of HLA-DR1 that corresponded to polymorphic changes in the P10 pocket (QuikChange mutagenesis system, Stratagene). For each reaction, a pLM1 [31] double-stranded vector carrying an insert of the β chain of HLA-DR1 was hybridized to two synthetic oligonucleotides primers, both containing the desired mutations. The oligonucleotides, each complementary to opposite strands of the vector, were extended during temperature cycling by PfuUltra HF DNA polymerase (Stratagene), without primer displacement. After the temperature cycling, the product was treated with DpnI endonuclease (Stratagene) to digest the parent DNA template and select for mutation-containing synthesized DNA. The vector DNA containing the desired mutations was transformed into XL1-Blue supercompetent cells (Stratagene). Sequencing of five randomly chosen clones revealed only the desired mutations.

To make HLA-DR1-βD57A, the primers used were 5′-GACGGAGC TGGGGCGGCCTGCTGCCGAGTATTGGAAC-3′ (sense) and 5′-GTT CCAATACTCGGCAGCAGGCCGCCCCAGCTCCGT-3′ (antisense). For HLA-DR1-βD57A/Y60H, the primers used were 5′-GAGCTGGGG CGGCCTGCTGCCGAGCACTGGAACAGCCAGAAGGAC-3′ (sense) and 5′-GTCCTTCTGGCTGTTCCAGTGCTCGGCAGCAGGCCGCC CCAGCTC-3′ (antisense). The primers for HLA-DR1-βD57V were 5′-GACGGAGCTGGGGCGGCCTGTGGCCGAGTATTGGAAC-3′ (sense) and 5′-GTTCCAATACTCGGCCACAGGCCGCCCCAGCTCCGTC-3′ (antisense). For HLA-DR1-βD57V/Y60S, 5′-GAGCTGGGGCGGCCTGTG GCCGAGTCTTGGAACAGCCAGAAGGAC-3′ (sense) and 5′-GTCCTT CTGGCTGTTCCAAGACTCGGCCACAGGCCGCCCCAGCTC-3′ (anti-

sense) were used. The HLA-DR1 mutants were expressed in *E. coli* inclusion bodies and refolded and isolated as described above for wild-type HLA-DR1.

Peptide Binding Assays

A standard peptide binding competition assay [26, 33–35] was used to determine binding affinities of peptides to the HLA-DR1 molecule and the mutants. Peptide-free wild-type HLA-DR1 produced in insect cells or a mutated form of HLA-DR1 produced in *E. coli* (25 nM) was mixed together with biotinylated Ha[306–318] peptide probe (Ha_{bio}, 25 nM) and varying concentrations of unlabeled competitor peptide (10^{-12}–10^{-5}M). The mixtures were incubated for 3 days at 37°C in 100 mM sodium phosphate buffer at pH 5.5, containing 50 mM NaCl, 1 mg/ml PMSF, 37 μg/ml iodoacetamide, 10 mM EDTA, 0.02% NaN_3, and 0.5 mg/ml octylglucoside, followed by detection of bound, biotinylated peptide using an immunoassay that employed anti-DR1 capture antibody LB3.1 and alkaline phosphatase-labeled streptavidin. IC_{50} values were obtained by fitting a binding curve to the plots of fluorescence versus concentration of competitor peptide. The IC_{50} value for the control Ha peptide included in each assay was 29 ± 14 nM (n = 8).

A direct binding assay was used to determine binding abilities of HLA-DR1 mutants. The assay was performed for 3 days at 37°C in the same buffer as described above; constant concentration of the proteins (25 nM) were used, and the range of concentrations of biotinylated peptides depended on the binding affinity of the particular peptide (10^{-11}–10^{-6} for tight binders and 10^{-11}–10^{-2} for weak binders). The incubation was followed by immunoassay as described above.

Crystallization

HLA-DR1 peptide bound complexes were prepared by incubating purified empty HLA-DR1 (1–5 μM) with at least 5-fold molar excess peptide for 3 days at 37°C in phosphate-buffered saline with 0.02% sodium azide. The complex was purified by gel filtration to remove aggregates and free peptide. Crystals of HLA-DR1/AAYSDQAT PLLLSPR complex were grown at room temperature by the vapor diffusion method in 10% polyethylene glycol 6000, 100 mM glycine (pH 4.0), with 1 μl precipitant solution mixed with 1 μl 10 mg/lL. For X-ray diffraction experiments, the crystal was soaked in mother liquor with 25% glycerol for 2 min and flashed cooled in liquid nitrogen. HLA-DR1 was isolated from insect cells.

For the HLA-DR1/AAYSDQATPLLLSPR/SEC3-3B2 crystal structure, purified HLA-DR1/AAYSDQATPLLLSPR complex was mixed in equimolar ratio with purified SEC3-3B2. Crystals of HLA-DR1/AAYSDQATPLLLSPR/SEC-3B2 were grown by the vapor diffusion method in hanging drops at 4°C under the following conditions: 2%–6% polyethylene glycol 4000, 5%–10% ethylene glycol, 100 mM sodium acetate (pH 5.2–5.6), with 1 μl precipitant solution mixed with 1μL 8 mg/ml protein complex. For X-ray diffraction experiments, the crystals were soaked for ~1 min in a cryoprotectant solution consisting of 25% ethylene glycol in the mother liquor and then flashed cooled in liquid nitrogen. The HLA-DR1 was purified from *E. coli*.

Data Collection and Processing

Diffraction data for HLA-DR1/AAYSDQATPLLLSPR was collected at the National Synchrotron Light Source (NSLS) with X25 beamline (λ = 1.10 Å) to a resolution of 2.4 Å.

A high-resolution data set (2.40 Å) of the HLA-DR1/AAYSD QATPLLLSPR/SEC3-2B2 complex was collected on a single crystal (300 μm × 200 μm × 200 μm) on an R-AXIS IV image plate detector with CuKα radiation. Collected data for both complexes were processed and scaled with Denzo, Scalepack, and the CCP4 package [36, 37].

Structure Determination

The structure of each complex was determined by molecular replacement. For the HLA-DR1/AAYSDQATPLLLSPR structure, coordinates from another complex of HLA-DR1 (Protein Data Bank code 1AQD) were used as the search model. After an initial rigid body refinement, five rounds of refinement included minimization, B factor, and minimization. A 2-fold noncrystallographic symmetry (NCS) averaging improved the quality of the electron density map.

In the case of HLA-DR1/AAYSDQATPLLLSPR/SEC3-2B2, coordinates for another complex of *E. coli*-derived HLA-DR1 and SEC3-3B2, carrying an N-methylated-designed peptide (Protein Data Bank code 1PYW) [26] were used as the search model to find a molecular replacement solution. Waters and the peptide were removed from the search model before use. After an initial rigid body refinement, eight rounds of refinement included minimization, B factor, and minimization.

For both structures, refinement was carried out with CNS [38], and manual inspection and rebuilding were carried out with XtalView [39]. Waters were added to the refined molecule by using CNS. The final models were verified for distortions on the secondary structure features with Procheck [40]. LSQKAB [41] was used to determine RMSD values for aligned coordinate sets.

MHC-Peptide Database Analysis

The SYFPEITHI database of known MHC binding peptides [18] and the IMGT HLA sequence database [15] were examined to find sets of similar HLA-DR1 alleles that differed in the P10 pocket residues and for which reliable motifs and many known peptide binders were available. HLA-DRB1*0401, HLA-DRB1*0404, and HLA-DRB1*0405 were selected for further analysis. HLA-DR allele-specific binding peptides from the SYFPEITHI databases generally were used without further alignment, although multiple-length variants of the same antigen and some ambiguous alignments were deleted. Residues predicted to bind into the P10 pocket were identified. A Fisher-Freeman-Halton Exact Test [42] revealed that the association between MHC alleles and residues at the P10 position approached significance (p = 0.056). To gain some insight into the nature of the allele specificity, residues were grouped by generic side chain properties: aromatic (Trp, Tyr, Phe), hydrophobic (Ile, Leu, Val, Met), small (Ala, Pro, Gly), polar (Thr, Ser, Cys, Asn, Gln), and a charged group (His, Glu, Arg, Lys, Asp), and the frequency of each group was calculated for each allele.

Supplemental Data

Supplemental Data including additional information regarding the crystal structures described and data/values used in the analysis of the P10 region of HLA-DR and the generation of figures are available at http://www.chembiol.com/cgi/content/full/11/10/1395/DC1.

Acknowledgments

We thank Stephen Baker (UMass Medical School) for assistance with statistical analysis. This work was supported by NIH-R01-AI38996 (L.J.S.) and NIH-F31-GM64859 (Z.Z.-R.). Research was carried out (in part) at the National Synchrotron Light Source, Brookhaven National Laboratory, which is supported by the U.S. Department of Energy, Division of Material Sciences and Division of Chemical Sciences, under Contract No. DE-AC02-98CH10886.

Received: May 19, 2004
Revised: July 9, 2004
Accepted: August 3, 2004
Published: October 15, 2004

References

1. Watts, C. (1997). Capture and processing of exogenous antigens for presentation on MHC molecules. Annu. Rev. Immunol. *15*, 821–850.
2. Chicz, R.M., Urban, R.G., Lane, W.S., Gorga, J.C., Stern, L.J., Vignali, D.A., and Strominger, J.L. (1992). Predominant naturally processed peptides bound to HLA-DR1 are derived from MHC-related molecules and are heterogeneous in size. Nature *358*, 764–768.
3. Rudensky, A., Preston-Hurlburt, P., Hong, S.C., Barlow, A., and Janeway, C.A., Jr. (1991). Sequence analysis of peptides bound to MHC class II molecules. Nature *353*, 622–627.
4. McFarland, B.J., and Beeson, C. (2002). Binding interactions

between peptides and proteins of the class II major histocompatibility complex. Med. Res. Rev. *22*, 168–203.
5. Corper, A.L., Stratmann, T., Apostolopoulos, V., Scott, C.A., Garcia, K.C., Kang, A.S., Wilson, I.A., and Teyton, L. (2000). A structural framework for deciphering the link between I-Ag7 and autoimmune diabetes. Science *288*, 505–511.
6. Fremont, D.H., Dai, S., Chiang, H., Crawford, F., Marrack, P., and Kappler, J. (2002). Structural basis of cytochrome c presentation by IE(k). J. Exp. Med. *195*, 1043–1052.
7. Ghosh, P., Amaya, M., Mellins, E., and Wiley, D.C. (1995). The structure of an intermediate in class II MHC maturation: CLIP bound to HLA-DR3. Nature *378*, 457–462.
8. Lee, K.H., Wucherpfennig, K.W., and Wiley, D.C. (2001). Structure of a human insulin peptide-HLA-DQ8 complex and susceptibility to type 1 diabetes. Nat. Immunol. *2*, 501–507.
9. Li, Y., Li, H., Martin, R., and Mariuzza, R.A. (2000). Structural basis for the binding of an immunodominant peptide from myelin basic protein in different registers by two HLA-DR2 proteins. J. Mol. Biol. *304*, 177–188.
10. Liu, X., Dai, S., Crawford, F., Fruge, R., Marrack, P., and Kappler, J. (2002). Alternate interactions define the binding of peptides to the MHC molecule IA(b). Proc. Natl. Acad. Sci. USA *99*, 8820–8825.
11. Southwood, S., Sidney, J., Kondo, A., del Guercio, M.F., Appella, E., Hoffman, S., Kubo, R.T., Chesnut, R.W., Grey, H.M., and Sette, A. (1998). Several common HLA-DR types share largely overlapping peptide binding repertoires. J. Immunol. *160*, 3363–3373.
12. Stern, L.J., Brown, J.H., Jardetzky, T.S., Gorga, J.C., Urban, R.G., Strominger, J.L., and Wiley, D.C. (1994). Crystal structure of the human class II MHC protein HLA-DR1 complexed with an influenza virus peptide. Nature *368*, 215–221.
13. O'Sullivan, D., Sidney, J., Del Guercio, M.F., Colon, S.M., and Sette, A. (1991). Truncation analysis of several DR binding epitopes. J. Immunol. *146*, 1240–1246.
14. Hammer, J., Takacs, B., and Sinigaglia, F. (1992). Identification of a motif for HLA-DR1 binding peptides using M13 display libraries. J. Exp. Med. *176*, 1007–1013.
15. Robinson, J., Waller, M.J., Parham, P., de Groot, N., Bontrop, R., Kennedy, L.J., Stoehr, P., and Marsh, S.G. (2003). IMGT/HLA and IMGT/MHC: sequence databases for the study of the major histocompatibility complex. Nucleic Acids Res. *31*, 311–314.
16. Tiwari, J.L., and Terasaki, P.I. (1981). HLA-DR and disease associations. Prog. Clin. Biol. Res. *58*, 151–163.
17. Sturniolo, T., Bono, E., Ding, J., Raddrizzani, L., Tuereci, O., Sahin, U., Braxenthaler, M., Gallazzi, F., Protti, M.P., Sinigaglia, F., et al. (1999). Generation of tissue-specific and promiscuous HLA ligand databases using DNA microarrays and virtual HLA class II matrices. Nat. Biotechnol. *17*, 555–561.
18. Rammensee, H., Bachmann, J., Emmerich, N.P., Bachor, O.A., and Stevanovic, S. (1999). SYFPEITHI: database for MHC ligands and peptide motifs. Immunogenetics *50*, 213–219.
19. Blythe, M.J., Doytchinova, I.A., and Flower, D.R. (2002). JenPep: a database of quantitative functional peptide data for immunology. Bioinformatics *18*, 434–439.
20. Sathiamurthy, M., Hickman, H.D., Cavett, J.W., Zahoor, A., Prilliman, K., Metcalf, S., Fernandez Vina, M., and Hildebrand, W.H. (2003). Population of the HLA ligand database. Tissue Antigens *61*, 12–19.
21. Fleckenstein, B., Kalbacher, H., Muller, C.P., Stoll, D., Halder, T., Jung, G., and Wiesmuller, K.H. (1996). New ligands binding to the human leukocyte antigen class II molecule DRB1*0101 based on the activity pattern of an undecapeptide library. Eur. J. Biochem. *240*, 71–77.
22. Yassai, M., Afsari, A., Garlie, J., and Gorski, J. (2002). C-terminal anchoring of a peptide to class II MHC via the P10 residue is compatible with a peptide bulge. J. Immunol. *168*, 1281–1285.
23. Anderson, M.W., and Gorski, J. (2003). Cutting edge: TCR contacts as anchors: effects on affinity and HLA-DM stability. J. Immunol. *171*, 5683–5687.
24. Madden, D.R., Gorga, J.C., Strominger, J.L., and Wiley, D.C. (1992). The three-dimensional structure of HLA-B27 at 2.1 Å resolution suggests a general mechanism for tight peptide binding to MHC. Cell *70*, 1035–1048.
25. Sundberg, E.J., Sawicki, M.W., Southwood, S., Andersen, P.S., Sette, A., and Mariuzza, R.A. (2002). Minor structural changes in a mutated human melanoma antigen correspond to dramatically enhanced stimulation of a CD4+ tumor-infiltrating lymphocyte line. J. Mol. Biol. *319*, 449–461.
26. Zavala-Ruiz, Z., Sundberg, E.J., Stone, J.D., DeOliveira, D.B., Chan, I.C., Svendsen, J., Mariuzza, R.A., and Stern, L.J. (2003). Exploration of the P6/P7 region of the peptide-binding site of the human class II major histocompatability complex protein HLA-DR1. J. Biol. Chem. *278*, 44904–44912.
27. Suri, A., Vidavsky, I., van der Drift, K., Kanagawa, O., Gross, M.L., and Unanue, E.R. (2002). In APCs, the autologous peptides selected by the diabetogenic I-Ag7 molecule are unique and determined by the amino acid changes in the P9 pocket. J. Immunol. *168*, 1235–1243.
28. Newton-Nash, D.K., and Eckels, D.D. (1993). Differential effect of polymorphism at HLA-DR1 beta-chain positions 85 and 86 on binding and recognition of DR1-restricted antigenic peptides. J. Immunol. *150*, 1813–1821.
29. Zarutskie, J.A., Sato, A.K., Rushe, M.M., Chan, I.C., Lomakin, A., Benedek, G.B., and Stern, L.J. (1999). A conformational change in the human major histocompatibility complex protein HLA-DR1 induced by peptide binding. Biochemistry *38*, 5878–5887.
30. Stern, L.J., and Wiley, D.C. (1992). The human class II MHC protein HLA-DR1 assembles as empty alpha beta heterodimers in the absence of antigenic peptide. Cell *68*, 465–477.
31. Frayser, M., Sato, A.K., Xu, L., and Stern, L.J. (1999). Empty and peptide-loaded class II major histocompatibility complex proteins produced by expression in *Escherichia coli* and folding in vitro. Protein Expr. Purif. *15*, 105–114.
32. Andersen, P.S., Lavoie, P.M., Sekaly, R.P., Churchill, H., Kranz, D.M., Schlievert, P.M., Karjalainen, K., and Mariuzza, R.A. (1999). Role of the T cell receptor alpha chain in stabilizing TCR-superantigen-MHC class II complexes. Immunity *10*, 473–483.
33. Hammer, J., Bono, E., Gallazzi, F., Belunis, C., Nagy, Z., and Sinigaglia, F. (1994). Precise prediction of major histocompatibility complex class II-peptide interaction based on peptide side chain scanning. J. Exp. Med. *180*, 2353–2358.
34. Jardetzky, T.S., Gorga, J.C., Busch, R., Rothbard, J., Strominger, J.L., and Wiley, D.C. (1990). Peptide binding to HLA-DR1: a peptide with most residues substituted to alanine retains MHC binding. EMBO J. *9*, 1797–1803.
35. Tompkins, S.M., Rota, P.A., Moore, J.C., and Jensen, P.E. (1993). A europium fluoroimmunoassay for measuring binding of antigen to class II MHC glycoproteins. J. Immunol. Methods *163*, 209–216.
36. Otwinowski, Z., and Minor, W. (1997). Processing of X-Ray diffraction data collected in oscillation mode. Methods Enzymol. *276*, 307–326.
37. CCP4 (Collaborative Computational Project) (1994). The CCP4 suite: programs for protein crystallography. Acta Crystallogr D Biol. Crystallogr. *50*, 760–763.
38. Brunger, A.T., Adams, P.D., Clore, G.M., DeLano, W.L., Gros, P., Grosse-Kunstleve, R.W., Jiang, J.S., Kuszewski, J., Nilges, M., Pannu, N.S., et al. (1998). Crystallography & NMR system: a new software suite for macromolecular structure determination. Acta Crystallogr. D Biol. Crystallogr. *54*, 905–921.
39. McRee, D.E. (1999). XtalView/Xfit–A versatile program for manipulating atomic coordinates and electron density. J. Struct. Biol. *125*, 156–165.
40. Laskowski, R.A., Moss, D.S., and Thornton, J.M. (1993). Main-chain bond lengths and bond angles in protein structures. J. Mol. Biol. *231*, 1049–1067.
41. Kabsch, W. (1978). A discussion of the solution for the best rotation to relate two sets of vectors. Acta Crystallogr. A *34*, 827–828.
42. Freeman, G.H., and Halton, J.H. (1951). Note on an exact treatment of contingency, goodness of fit and other problems of significance. Biometrika *38*, 141–149.
43. DeLano, W.L. (2002). The PyMol Molecular Graphics System (San Carlos, CA: DeLano Scientific).